Summer Student Program Report

Beam Impedance Studies of the PS Beam Gas Ionization Monitor

Beams and RF Studies Section
Radio Frequency Group
BEAMS Department

(BE-RF-BR)

Author:
Fotios Avgidis

Supervisors:
Christine Vollinger
Thomas Roland Kaltenbacher

September 30, 2016

Abstract

The Beam Gas Ionization monitor (BGI) is a device for continuous beam size monitoring that is intended to be installed in the CERN Proton Synchrotron (PS) during the extended year-end technical stop from December 2016 to April 2017. With the objective of determining the impedance contribution of the BGI vacuum chamber to the overall beam impedance, we report on RF measurements on the device in a laboratory frame, measurement data analysis, and RF simulations of the structure under investigation.

For the impedance contribution characterization of the BGI, the following approach has been followed: First, the EM fields inside a simplified BGI model that doesn't include any of the internal components of the vacuum chamber have been simulated. RF measurements have been performed on the same empty structure showing great agreement between measurement and simulation and thus verifying the validity of the model. Second, simulations have been executed on a fully assembled BGI model that includes all the internal elements of the BGI vacuum chamber with the purpose of including the impedance contribution of the BGI to the PS impedance model.

1 Introduction

The CERN Proton Synchrotron (PS) belongs to the Large Hadron Collider (LHC) injector chain. Its main role is to contribute to the acceleration of particle beams for the LHC. It usually accelerates either protons delivered by the Proton Synchrotron Booster or heavy ions from the Low Energy Ion Ring (LEIR) and feeds them to the Super Proton Synchrotron (SPS) where the particles are being further accelerated and then fed directly to the LHC for collision. In the framework of the LHC Injectors Upgrade project, important hardware changes are foreseen in the CERN Proton Synchrotron [1]. This includes the addition of Beam Gas Ionization monitors (BGI) to the PS. The task of this device is to measure the transverse beam size of all the different particle beams that can be accelerated in the PS. The design of the BGI for the PS constitutes an upgrade on the current BGI for the LHC and the SPS.

Inside the beam pipe of the BGI, the interaction between the beam field and any structural discontinuities of the BGI can generate electromagnetic fields localized in particular regions. These fields constitute a mode. Longitudinal modes produce narrow peaks in the coupling impedance spectrum along the direction of propagation. Usually modes with a frequency below cut-off, that do not propagate through the beam pipe, produce more pronounced impedance peaks. Since resonances can be a potential source of beam instabilities in the accelerator, it is necessary to first simulate by means of an EM solver the beam-coupling impedance and the properties of the BGI modes and then verify these results by performing RF measurements on the device in a laboratory frame before installing the BGI in the CERN Proton Synchrotron [2].

2 Beam Gas Ionization Monitor

The Beam Gas Ionization monitor (BGI) measures the transverse size of the particle beam by monitoring the position of the electrons produced after the ionization of Neon gas. Two electrodes of the opposite polarity installed across each other on the top and bottom of the BGI cage separate the negatively charged electrons from the positively charged ions produced during the ionization. These top and bottom electrodes are creating a vertical electric field that guides the electrons towards a detector, while electrodes installed on the sides of the cage are limiting the field leakages. An applied external magnetic field confines the electron movement by reducing their transverse spread. Opposite of the detector, an ion trap is installed in order to capture the ions produced during the gas ionization, to avoid free ions causing a secondary emission of ions and electrons when reaching an electrode (see figure 2.1). A picture of the BGI is shown in figure 2.2. The CAD model of the BGI and a cutaway view of its vacuum chamber with its internal components embedded inside are depicted in figure 2.3.

To measure the electron distribution, a hybrid pixel detector is used. It consists of a CMOS pixel detector readout chip (Medipix3) connected to a segmented semiconductor sensor. When an electron hits the surface of the sensor it deposits all of its charge locally. This charge is then collected by the nearest pixels of the detector.

Each pixel contains individual amplification and control circuitry [3]. An aluminum honeycomb mesh is installed on top of the detector to ensure shielding against EM fields. The detector is cooled down to zero degrees Celsius using a copper plate installed behind it.

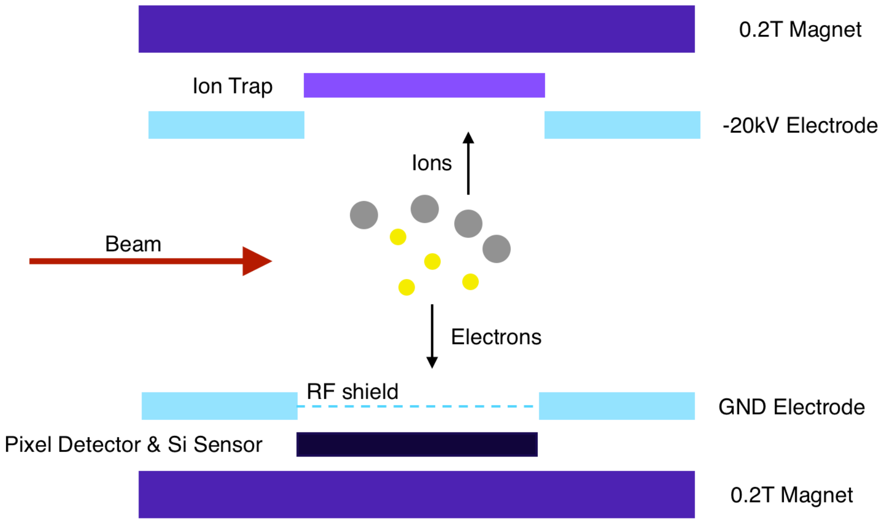

Figure 2.1: Model of the internal BGI layout. Not shown here the electrodes on the sides of the cage (parallel to the page) that limit the field leakage.

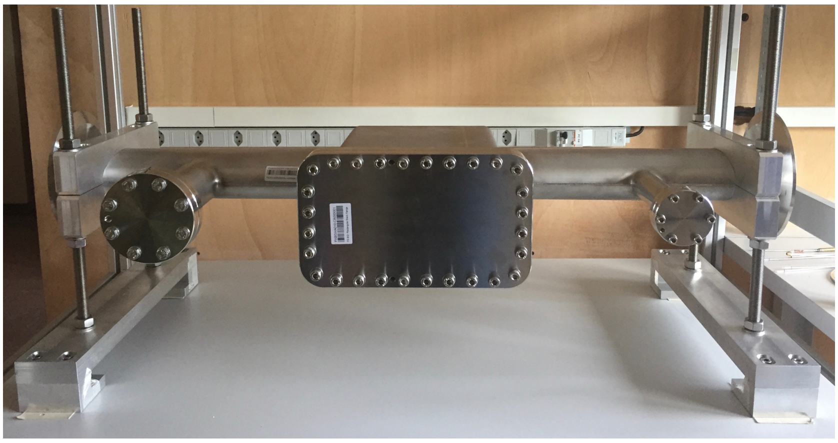

Figure 2.2: The BGI mounted on a frame. Its vacuum chamber and beam pipe are visible.

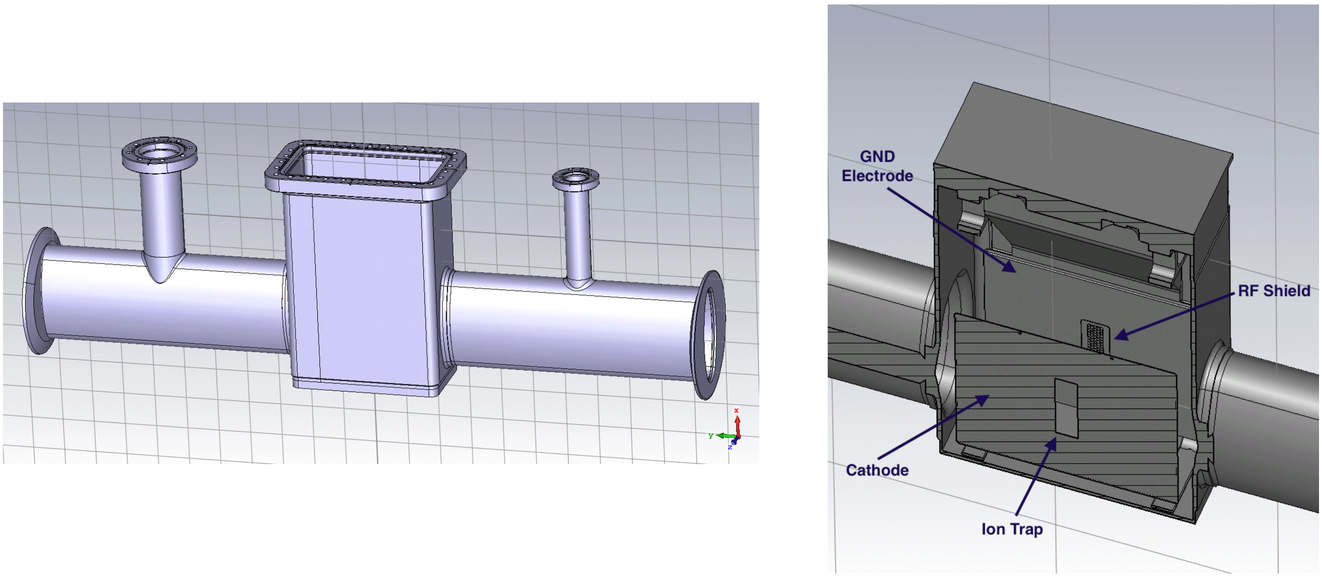

Figure 2.3: Left: CAD model of the design. Right: cutaway view of the fully assembled BGI vacuum chamber.

3 Simulation

To evaluate the BGI in terms of its EM properties, simulations were performed initially on a simplified structure, where the vacuum chamber of the BGI doesn't include any internal components (figure 3.1). For all simulation needs, the electromagnetic field simulation software CST STUDIO SUITE 2016 was employed. The simulation of the electromagnetic field is achieved numerically by discretizing the structure space using a tetrahedral mesh and then solving the Maxwell equations for each mesh cell. Three different types of simulation were performed: eigenmode simulation, frequency domain simulation, and wakefield simulation.

3.1 Eigenmode Simulation

In order to perform an eigenmode simulation, we have closed all open boundaries of the BGI model. In a closed structure without any excitations sources, each solution of the Maxwell Equation corresponds to a resonant mode, with its eigensolution corresponding to the eigenfrequency of the mode. From the eigenmode simulation we can obtain the frequency of each mode, the corresponding field configuration, as well as parameters relevant to the coupling impedance: The quality factor, the R-over-Q, and the shunt Impedance [4].

The quality factor (Q) is a dimensionless quantity characteristic for every harmonic oscillator and it is defined as:

$$Q = \frac{f_{resonant}}{\Delta f} = \frac{\omega U}{P} \qquad (1.1)$$

Where $f_{resonant}$ is the frequency of the resonant mode and Δf is the bandwidth at the -3dB point. U is the energy stored in the structure and P, its power loss. Higher Q values correspond to a lower rate of energy loss relative to the stored energy.

The R-over-Q is a relation between the voltage developed along a given path to the energy required to produce this voltage:

$$\frac{R}{Q} = \frac{|V_{accelerating}|^2}{2\omega U} \quad (1.2)$$

Where $V_{accelerating}$ is the voltage "seen" by the accelerating particles in the beam and U, the energy stored in the structure. The R-over-Q is measured in Ohms since Q is dimensionless. The $V_{accelerating}$ is defined as:

$$V_{accelerating} = \int_{-\infty}^{\infty} E_z e^{j\frac{\omega}{\beta c}z} dz \quad (1.3)$$

Where β is the transit-time factor and it equals to the ratio of the speed of the particle and the speed of light, and z is the path traveled by the particle.

Finally, the shunt impedance is the product of the R-over-Q and the quality factor Q. Combining equations (1.1) and (1.2) leads to:

$$R = \frac{|V_{accelerating}|^2}{2U} \quad (1.4)$$

The results from the eigenmode simulation on the empty BGI structure are summarized in the left side of table 3.1.

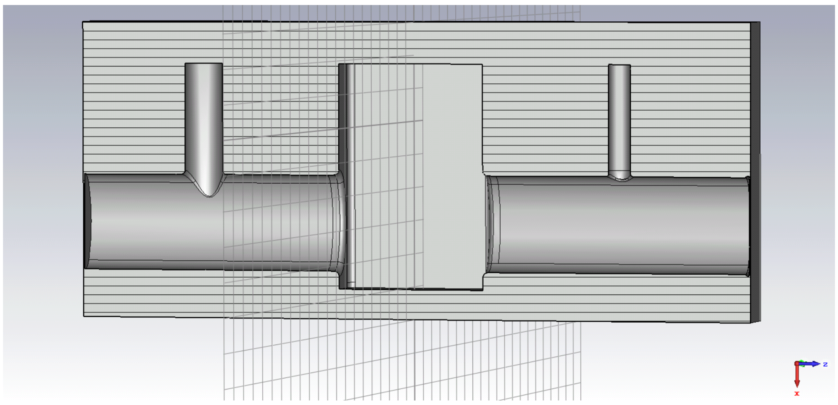

Figure 3.1: Cutaway view of the simplified BGI model used for the eigenmode simulation. All the internal features shown in figure 2.3 have been omitted for this simulation. The curvature of the model has been reduced to simplify the meshing of the structure.

3.2 Frequency Domain Simulation

From the frequency domain simulation, the S-parameters of the structure were determined. The S-parameters describe the electrical behavior of the structure as a power ratio between two or more ports. The calculation of the S-parameters was achieved by modeling two measurement probes on both sides of the BGI beam pipe (figure 3.2) and defining a waveguide port on the end of each probe. The probes were modeled as a coaxial structure with aluminum core and shield, and a Teflon insulator between them. The goal of this model is to mimic as accurately as possible the probe measurement described in the next paragraph. The transmission parameter that was studied mainly was S_{21} (the forward transmission coefficient) which corresponds to an excitation on port 1 and a transmission measurement on port 2. S_{21} is identical to S_{12} in a passive system like ours. The magnitude plot for S_{21} is shown in figure 3.3.

3.3 Wakefield Simulation

Finally, from the wakefield simulation, the wake potential inside the structure was calculated. The wake potential is the energy induced by the electric field of the lead particle of the beam on a unit charge trailing particle that follows the lead particle at a constant distance through the entire structure [5]. To simulate the wake potential, the beam entrance and exit planes in the model shown in figure 3.1 were defined as open boundaries. The wakefield simulation is performed in the time domain. The frequency domain equivalent of the wake potential is the beam-coupling impedance. To obtain the impedance spectrum, a Fourier transform is performed on the wake potential. The coupling impedance is of particular interest since narrow peaks in the impedance spectrum can be a potential source of beam instabilities. The calculated beam-coupling impedance spectrum of the BGI vacuum chamber is shown in figure 3.4. In order to extract the impedance peaks from the spectrum, a MATLAB script that detects changes in the monotonicity of the impedance spectrum was used (see appendix). Furthermore, the quality factor and the R-over-Q of each mode were calculated using a method similar to the one described in the next paragraph. The mode frequencies with their corresponding parameters are shown in table 3.2.

4 Measurements

For the last step of the evaluation, measurements were performed on the empty BGI structure. Two measurement probes were installed on both sides of the BGI beam pipe and S-parameter measurements were carried out using a vector network analyzer (Agilent Technologies E5071C). A weak coupling to each mode was assured by adjusting the penetration of the probes inside the beam pipe of the BGI. The measured forward transmission coefficient S_{21} is shown in figure 3.5 where the resonant modes appear as an amplitude peak. It is therefore possible to determine the quality factor of each mode using the first part of equation 1.1. For this, a MATLAB script that plots the measurement data and calculates the quality factor for every mode was developed (see appendix). The main function of the script is to remove unwanted noise from the spectrum, detect peaks in its magnitude, calculate the -3dB bandwidth of each peak, and finally, calculate the quality factor. The measured mode frequencies and their quality factors are presented in the right side of table 3.1.

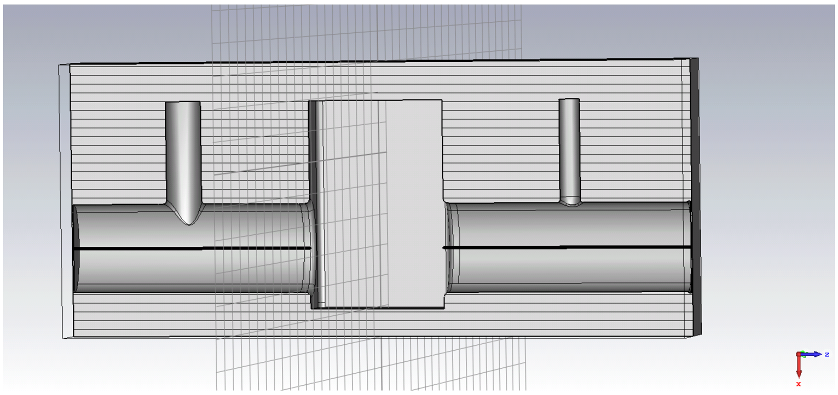

Figure 3.2: Cutaway view of the simplified BGI model with the inclusion of measurement probes on both sides of the beam pipe.

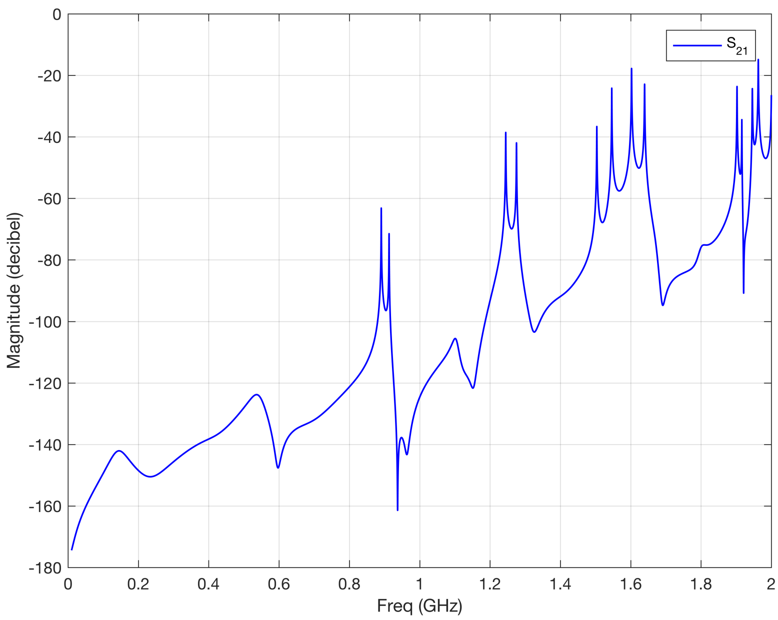

Figure 3.3: Magnitude plot of the forward transmission coefficient (S_{21}) simulation. Resonant modes appear in the waveform as an amplitude peak.

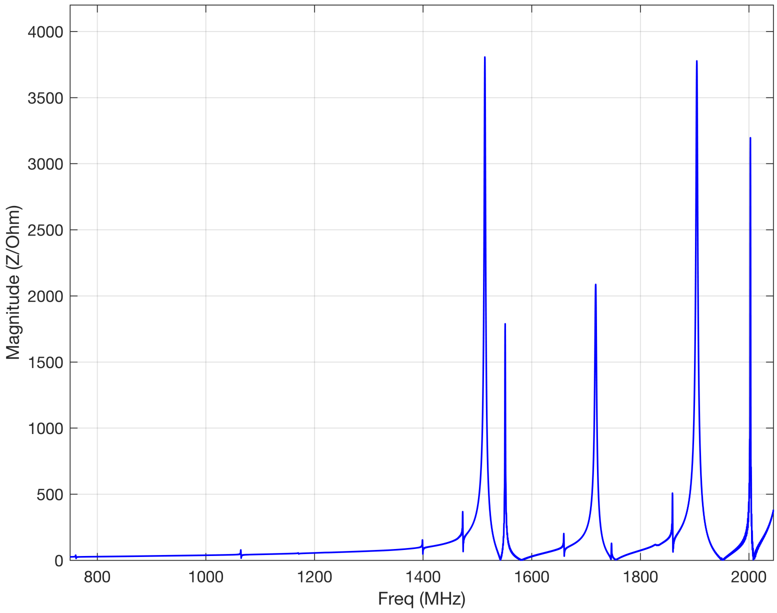

Figure 3.4: Magnitude plot of the wake impedance spectrum. The impedance is a measure of the interaction of the particle beam with its environment. Sharp peaks in the impedance are visible on higher frequencies.

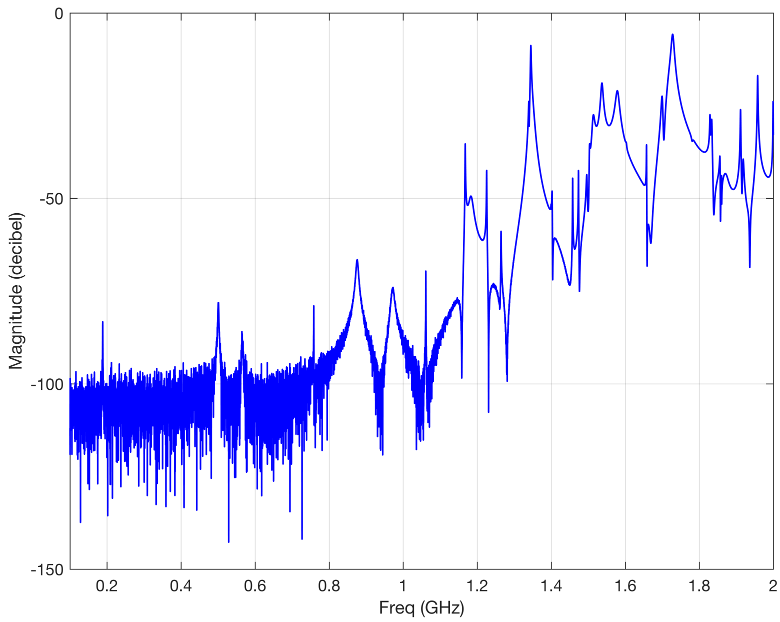

Figure 3.5: Magnitude plot of the forward transmission coefficient (S_{21}) measurement. Lower frequencies suffer from noise. Mode resonant frequencies and their quality factors can be extracted from this measurement.

	Eigenmode Simulation (Tetrahedral Mesh)				Probe Measurements	
Mode	Frequency (MHz)	R/Q β=1 (Ω)	Shunt Impedance β=1 (Ω)	Q Factor	Frequency (MHz)	Q Factor
1	761.0	1.04E-02	3.92E+01	3772	758.5	3456
2	1065.1	2.02E-02	9.35E+01	4637	1061.3	4157
3	1171.7	8.51E-03	2.62E+01	3084	1168.2	2931
4	1233.0	1.02E-02	2.91E+01	2866	1227.2	2129
5	1266.5	2.66E-03	8.21E+00	3086	1265.2	1577
6	1343.2	1.26E-04	5.49E-01	4350	1340.4	1310
7	1345.3	6.92E-02	2.24E+02	3242	1345.6	3998
8	1399.9	2.54E-02	1.17E+02	4615	1402.8	1341
9	1408.7	5.01E-04	1.90E+00	3796	-	-
10	1464.5	1.06E-02	5.94E+01	5614	1457.8	3163
11	1473.9	7.82E-02	3.23E+02	4130	1473.7	3199
12	1505.3	1.63E+00	6.82E+03	4174	1504.4	1567
13	1508.9	2.09E+00	8.75E+03	4194	-	-
14	1523.0	2.10E+00	8.00E+03	3809	1522.4	2002
15	1551.9	8.73E-01	4.75E+03	5442	1554.2	4563
16	1613.5	1.13E-04	5.07E-01	4469	-	-
17	1660.2	4.71E-02	1.97E+02	4181	1657.2	3357
18	1707.0	1.51E+00	6.75E+03	4466	1699.7	500
19	1726.7	1.95E+00	8.95E+03	4583	1729.4	1617
20	1748.7	2.47E-02	1.40E+02	5691	-	-
21	1793.0	9.79E-02	4.64E+02	4736	-	-
22	1831.9	3.45E-02	2.23E+02	6457	1829.3	1430
23	1840.8	3.87E-02	2.23E+02	5772	1835.1	3576
24	1861.4	1.49E-01	8.07E+02	5431	1860.1	2709
25	1868.8	3.65E-04	2.38E+00	6522	-	-
26	1906.8	5.56E+00	2.33E+04	4195	1907.7	3120
27	1917.3	3.85E-04	1.81E+00	4698	1918.5	599
28	1947.2	3.09E-03	1.60E+01	5163	-	-
29	1952.0	4.46E-03	2.06E+01	4614	1953.6	3491
30	2004.4	8.85E-01	4.47E+03	5052	1998.1	3561

Table 3.1: Left: Summary of the eigenmode simulation results of the empty BGI structure Right: the frequency of the resonant modes in the measured waveform (figure 3.5) and their corresponding calculated quality factors.

Wake Impedance (Z-direction)

Frequency (MHz)	R/Q β=1 (Ω)	Coupling Impedance (Ω)	Q Factor
760.72	4.82E-02	3.87E+01	803
1064.43	5.70E-02	8.01E+01	1406
1170.37	2.21E-01	5.53E+01	251
1399.24	1.07E-01	1.54E+02	1443
1473	2.16E-01	3.68E+02	1704
1513.85	5.81E+00	3.81E+03	656
1551.09	1.05E+00	1.83E+03	1739
1659.2	1.11E-01	2.03E+02	1825
1717.77	3.49E+00	2.09E+03	599
1747.03	4.86E-02	1.41E+02	2905
1859.51	2.21E-01	5.28E+02	2393
1904.1	5.89E+00	3.78E+03	642
2002.71	1.10E+00	3.33E+03	3024

Table 3.2: The frequency and the coupling impedance of the modes in the wake impedance spectrum (figure 3.4).

5 Discussion of Results

The main method of benchmarking the simulation data is comparing the simulated eigenmodes with the modes extracted from the measured magnitude plot of the forward transmission coefficient S_{21}. In that respect, we see an excellent agreement between the two sets of resonant frequencies. In total, 23 out of the 30 simulated modes were also found in the forward transmission measurement. The deviation between the frequency of simulated and measured modes is systematically in the range of a few MHz, with the average deviation between the two frequencies being 1.84 MHz (an error of 2.46%). From the set of the seven simulated modes that we were unable to measure, the electric field of modes 20 and 25 was found to have a negligible magnitude in the beam pipe where the measuring probes are installed. Similarly, mode 13 has a negligible electric field in one side of the beam pipe, making the coupling of the probe on that side very challenging. There were indications that mode 21 was present in the measurements, but the coupling of the probes to it was exceedingly weak for a reliable measurement. Modes 9 and 28 have a simulated frequency that almost coincides with the measured frequency of another mode (namely the frequency of modes 8 and 29, respectively), which is an indication of a possible superposition of modes in the measured waveform. Finally, mode 16 has an insignificant simulated impedance, which can be a possible justification of our incapacity to detect it.

A more significant deviation was found between the measured and the simulated quality factors of each mode. The measured modes have, as expected, a smaller quality factor than the simulated modes. This is a phenomenon often observed in cavity measurements. It can be attributed to a number of factors, such as cavity field leakage, material losses, or exceedingly strong or weak coupling between the mode and the measurement probes. Furthermore, due to engineering tolerances, it is possible that the geometry of the simulation model doesn't coincide entirely with the actual structure. Finally, particular parameters, such as the permeability and the conductivity of the material, or the surface resistance of the structure are subject to external factors that are not taken into account in the simulation (such as temperature, or mechanical stress).

On the lower measured frequency spectrum (10 to 700 MHz), modes that do not appear on the eigenmode simulation are visible. Due to the high noise content of these frequencies it was not possible to reliably extract their resonance frequency or quality factor. These modes are well below the cutoff frequency of the structure, which from the frequency domain simulation was found to be 1200 MHz. Therefore, these modes do not propagate through the beam pipe. Their nature can be attributed to the field variations due to the presence of the measurement probes. Indeed, a second eigenmode simulation was performed, this time in a BGI model with the probes included (figure 2.2), and a number of modes with a resonance frequency lower than 700 MHz were present.

From the forward transmission coefficient simulation (figure 3.3) we were able to extract 12 modes (not shown here), 5 of which show an excellent agreement with the modes found in the eigenmode simulation and the measurement, while for the other 7 modes there is evidence that they are caused by the field alterations due to the probes penetrating the beam pipe. Indeed, in the eigenmode simulation with the probes included, all 7 modes where present. The average deviation between the frequencies extracted from the forward transmission coefficient simulation and their corresponding eigenmode simulation frequencies was calculated to be 0.25 MHz (an error of approximately 0.037%). Not all measured modes could be seen in this frequency domain simulation since the position of the probes inside the beam pipe is fixed for the simulation (no parametric study was performed), while during the measurement the penetration of the probes was adjusted to ensure sufficiently low coupling to the mode.

Finally, we compare the wakefield simulation results to the results obtained by the measurement. We again see an excellent agreement between the simulated and measured frequencies with an average deviation of 5.4 MHz (which corresponds to an error of 1.09%). Since the wakefield simulation is performed on a model with open boundaries, no standing wave modes appear on this simulation. This is the reason why some of the measured modes do not appear in the simulation.

By comparing the wakefield simulation to the eigenmode simulation, we see an excellent agreement between the two frequency sets. As expected, the modes with high coupling impedance in the Wakefield simulation correspond to modes with high shunt impedance in the eigenmode simulation. The extracted quality factors of each wakefield mode are not in complete agreement with the quality factors of the eigenmode simulation. This is attributed to the lower frequency resolution used in the wakefield simulation, resulting in the undersampling of the impedance spectrum. As mentioned earlier, the wakefield simulation is performed in the time domain and it is a time intensive process. Achieving the same frequency resolution with the eigenmode simulation would requires unrealistically long simulation times. The same deviation between eigenmode and wakefield simulations is observed for the R-over-Q value of each mode. This is expected since the R-over-Q is extracted by dividing the coupling impedance by the quality factor.

In total, six modes appear to have high coupling impedance to the beam (impedance larger than 500 Ω) and can potentially have a negative effect on the beam. These modes are summarized in table 3.3 together with their corresponding modes from the eigenmode simulation. High impedance in general can lead to higher beam emittance (spread of the beam particles), beam instabilities, and even beam loss. The exact effect of these high-impedance modes on the stability of the beam needs to be evaluated by using these simulated results as an input for beam-dynamics studies.

Eigenmode Simulation (Tetrahedral Mesh)			Wake Impedance (Z-direction)	
Mode	Frequency (MHz)	Shunt Impedance β=1 (Ω)	Frequency (MHz)	Coupling Impedance (Ω)
13	1508.88	8748.57	1513.85	3814.85
14	1522.99	7997.36		
15	1551.89	4752.77	1551.09	1831.18
18	1706.98	6751.89	1717.77	2090.42
19	1726.69	8948.00		
24	1861.45	807.34	1859.51	528.48
26	1906.80	23339.85	1904.1	3777.97
30	2004.37	4470.00	2002.71	3329.25

Table 3.3: High impedance modes. In two cases, two separate modes from the eigenmode simulation appeared as a superposition of modes in the wakefield simulation. This can be attributed to the lower sampling rate used in the wakefield simulation.

6 Conclusion & Outlook

In this project, we have characterized the beam coupling impedance of a beam gas ionization monitor for the CERN Proton Synchrotron (PS). Simulations with CST STUDIO SUITE 2016, together with RF measurements have been performed. Simulation and measurement results are in great agreement.

The simulation results on the fully assembled BGI model that includes all the internal elements of the BGI vacuum chamber were not included since due to time limitations it wasn't possible to verify the results with probe measurements.

In continuation of this project, a number of improvements can be made, particularly in the experimental domain. In addition to the probe measurement, impedance measurements could also be performed using the coaxial wire method. In that measurement, a metallic wire that acts as a transmission line is stretched inside the BGI. The wire excites the structure with an electromagnetic field similar to the field generated by an ultra-relativistic point charge [6]. Using this method, the forward transmission coefficient waveform can be measured using a network analyzer. Furthermore, the probe measurement could be improved with the addition of absorption foam at the ends of the beam pipe. This would suppress reflections and reduce the noise of the measurements. Finally, a thermal simulation could be carried out to predict any possible unwanted heating effects due to electric field built up inside the structure, particularly near the pixel detector.

7 Acknowledgments

I would like to thank my supervisors, Christine Vollinger and Thomas Kaltenbacher for their guidance, help with the simulations and measurements, and their valuable feedback on this report. I would also like to thank Patrick Krämer for the interesting discussions regarding the measurements. Last but not least, I would like to thank the entire BR section for making me feel welcomed during my summer assignment.

REFERENCES

[1] M. Migliorati, et al., "Beam-wall interaction in the CERN Proton Synchrotron for the LHC upgrade," Physical Reviews, vol. 16, no. 3, pp. 0310011-0310111, 2013.

[2] M. M. S. Persichelli, "Beam coupling impedance simulation and RF measurements of a passive extraction septum for particle absorbing in the CERN Proton Synchrotron," in XX Riunione Nazionale di Elettromagnetismo, Padua, Italy, 2014.

[3] R. Ballabriga, et al., "Medipix3: A 64 k pixel detector readout chip working in single photon counting mode with improved spectrometric performance," Nuclear Instruments and Methods in Physics Research, vol. A, no. 633, pp. 15-18, 2011.

[4] E. Jensen, "Computational Tools for RF Structure Design," in Joint USPAS-CAS-Japan-Russia Accelerator School on Physics and Technology of Linear Accelerator Systems, Long Beach, CA, USA, 2003.

[5] K. Bane, "wakefield effects in a linear collider," in U.S. Summer School on High Energy Particle Accelerators, Batavia, Illinois, USA, 1984.

[6] A. Mostacci et al., "RF coupling impedance measurements versus simulations", in Beam Dynamics in Future Hadron Colliders and Rapidly Cycling High-Intensity Synchrotrons, Geneva, Switzerland, 2004.

APPENDIX

The MATLAB script used for the extraction of the coupling impedance and frequency values (table 3.2) and the plotting of the wakefield spectrum is attached bellow:

```
clear all;
clc

format shortg;

filename = '';
delimiterIn = ' ';
headerlinesIn = 2;

A = importdata(filename,delimiterIn,headerlinesIn);

Impedance = A.data(:,2);
Freq = A.data(:,1);

Peaks_Imp = findpeaks(Impedance);

M = [];

for i = (1:length(Peaks_Imp));
pks = Peaks_Imp(i);
[tolerance, location_peak] = min (abs(pks - Impedance));
freq_peak_loc_imp = Freq(location_peak);
M = [M;freq_peak_loc_imp];
end

Peaks = horzcat(Peaks_Imp,M)

fig1 = figure('name','Wake (Coupling) Impedance in Z-direction');
h = plot(Freq, Impedance);
set(h, 'Color', 'blue','LineWidth',1);
xlabel('Freq (MHz)');
ylabel('Magnitude (Z/Ohm)');
grid on;
print -r600 -dpng wakefield.png
```

The MATLAB script for the calculation of the quality factors of the measured modes (table 3.2) and the plotting of the measurement data is given bellow:

```
clear all;
close all;
clc

filename = '';

%Data Extraction & Plotting

data = read(rfdata.data, filename);
freq = data.Freq;

s_params = extract(data,'S_PARAMETERS',50);

s11 = s_params(1,1,:);
```

```
s22 = s_params(2,2,:);
s12 = s_params(1,2,:);
s21 = s_params(2,1,:);

fig1 = figure('name','Smith Chart Reflection');
hold off;
h = smith(data,'S11');
set(h, 'Color', 'red','LineWidth',2);
hold on;
i = smith(data,'S22');
set(i,'Color', 'blue','LineWidth',2,'LineStyle',':');
l1 = legend;
legend('S_{11}', 'S_{22}');
legend show;
hold off;

fig2 = figure('name','Smith Chart Transmission');
hold off;
h = smith(data,'S21');
set(h, 'Color', 'red','LineWidth',2);
hold on;
i = smith(data,'S12');
set(i,'Color', 'blue','LineWidth',2,'LineStyle',':');
l2 = legend;
legend('S_{21}', 'S_{12}');
legend show;
hold off;

fig3 = figure('name','Magnitude Plot Reflection');
hold off;
h = plot(data,'S11', 'db');
set(h, 'Color', 'red','LineWidth',2);
hold on;
i = plot(data,'S22','db');
set(i,'Color', 'blue','LineWidth',2,'LineStyle',':');
l3 = legend;
legend('S_{11}', 'S_{22}');
legend show;
hold off;

fig4 = figure('name','Magnitude Plot Transmission');
hold off;
h = plot(data,'S21','db');
set(h, 'Color', 'red','LineWidth',2);
hold on;
i = plot(data,'S12','db');
set(i,'Color', 'blue','LineWidth',2,'LineStyle',':');
l4 = legend;
legend('S_{21}', 'S_{12}');
legend show;
hold off;

%Q Factor Calculation

s21_dB = 20*log10(abs(s21(:)));
a_limit = 1*10^9; %Adjust accordingly
b_limit = 2*10^9; %Adjust accordingly
range = a_limit:10^2:b_limit;

fit=pchip(freq,s21_dB,range);
fit_smooth = smooth(fit,100,'lowess');
```

```matlab
%Adjust the span and the resolution accordingly

Loss_fit = max(fit_smooth);
Resonance_fit = range(fit_smooth == max(fit_smooth))

ymarker1 = Loss_fit;
xmarker1 = Resonance_fit;

threedB = Loss_fit - 3;

location_Loss_fit = find(fit_smooth == Loss_fit);

fit_limit_a = fit_smooth(range == a_limit);
location_fit_limit_a = find(fit_smooth == fit_limit_a);
fit_low = fit_smooth(location_fit_limit_a:location_Loss_fit);

fit_limit_b = fit_smooth(range == b_limit);
location_fit_limit_b = find(fit_smooth == fit_limit_b);
fit_high = fit_smooth(location_Loss_fit:location_fit_limit_b);

lowfreq = range(range < Resonance_fit);
[tolerance_low, location_low] = min (abs(fit_low-threedB));
corner_low_fit = lowfreq(location_low)

ymarker2 = threedB;
xmarker2 = corner_low_fit;

highfreq = range(range >= Resonance_fit);
[tolerance_high, location_high] = min (abs(fit_high-threedB));
corner_high_fit = highfreq(location_high)

ymarker3 = threedB;
xmarker3 = corner_high_fit;

Resonance_middle = (corner_low_fit + corner_high_fit)/2;
[tolerance_middle_amp, location_mid_amp] = min (abs(range-Resonance_middle));
Resonance_middle_amp = fit_smooth(location_mid_amp);

ymarker4 = Resonance_middle_amp;
xmarker4 = Resonance_middle;

bandwidth = abs (corner_low_fit - corner_high_fit);
Q = (Resonance_middle / bandwidth)

fig5 = figure('name','S21 Fit');
plot(range,fit_smooth,freq,s21_dB,xmarker1,ymarker1,'bo',xmarker2,ymarker2,'bo',
xmarker3,ymarker3,'bo',xmarker4,ymarker4,'b*');
hold on;
line = plot([xmarker2 xmarker3], [ymarker2 ymarker3]);
set(line,'Color', 'blue','LineWidth',1,'LineStyle',':');
xlabel('Freq (Hz)');
ylabel('Magnitude (decibel)');
axis([a_limit,b_limit,(threedB - 2),(Loss_fit + 1)]);
grid on;
print -r600 -dpng fit.png
```